



Annual Review of Condensed Matter Physics
 From Stochastic
 Thermodynamics to
 Thermodynamic Inference

Udo Seifert

Institut für Theoretische Physik, Universität Stuttgart, 70550 Stuttgart, Germany;
 email: useifert@theo2.physik.uni-stuttgart.de

Annu. Rev. Condens. Matter Phys. 2019. 10:171–92

The *Annual Review of Condensed Matter Physics* is
 online at conmatphys.annualreviews.org

<https://doi.org/10.1146/annurev-conmatphys-031218-013554>

Copyright © 2019 by Annual Reviews.
 All rights reserved

Keywords

nonequilibrium, entropy production, active particles, thermodynamic
 uncertainty relation, efficiency of molecular motors

Abstract

For a large class of nonequilibrium systems, thermodynamic notions like work, heat, and, in particular, entropy production can be identified on the level of fluctuating dynamical trajectories. Within stochastic thermodynamics various fluctuation theorems relating these quantities have been proven. Their application to experimental systems requires that all relevant mesostates are accessible. Recent advances address the typical situation that only partial, or coarse-grained, information about a system is available. Thermodynamic inference as a general strategy uses consistency constraints derived from stochastic thermodynamics to infer otherwise hidden properties of nonequilibrium systems. An important class in this respect are active particles, for which we resolve the conflicting strategies that have been proposed to identify entropy production. As a paradigm for thermodynamic inference, the thermodynamic uncertainty relation provides a lower bound on the entropy production through measurements of the dispersion of any current in the system. Likewise, it quantifies the cost of precision for biomolecular processes. Generalizations and ramifications allow the inference of, inter alia, model-free upper bounds on the efficiency of molecular motors and of the minimal number of intermediate states in enzymatic networks.



1. INTRODUCTION

Stochastic thermodynamics provides a conceptual and quantitative framework for describing the wide class of fluctuating nonequilibrium systems that are coupled to, or even embedded in, a heat bath of well-defined temperature (1). This condition holds for many soft-matter systems and biosystems, and, in particular, for experiments on the single molecule, or single colloidal particle, level. It can also be realized for transport problems through single-electron boxes (2). For such systems, the notions of classical thermodynamics, like work, heat, and entropy production, are identified on the level of individual, fluctuating trajectories taken from well-defined nonequilibrium ensembles. One prominent example, and, in fact, one of the pillars of this field, is the Jarzynski relation that relates a nonlinear average of the fluctuating work exerted on an initially thermally equilibrated system by changing a control parameter to the free energy difference between the equilibrium states associated with the initial and the final value of this control parameter (3). Thus, an equilibrium property, the free energy difference, can be inferred from experiments that may drive the system deeply into nonequilibrium. Such an exact relation, valid beyond any linear response regime, came as quite a surprise in 1997. A comprehensive review of the Jarzynski relation including its important generalization by Crooks (4, 5) has been published in this journal (6). The Jarzynski relation does not require the identification of heat, let alone entropy production, on the level of individual trajectories. For heat, such an identification was suggested in References 7 and 8 by Sekimoto, and for the various contributions to entropy production in Reference 9. This approach based on stochastic dynamics for a system coupled to a heat bath, later called stochastic thermodynamics, also offered an additional perspective on the famous fluctuation theorem (FT) that quantifies the probability of trajectories with negative total entropy production first derived in the long-time limit for thermostatted and chaotic dynamics (10–12) and then for stochastic dynamics (13, 14).

From the present perspective, one could argue that in this initial phase of the development of stochastic thermodynamics the focus was identifying the thermodynamic notions along trajectories and deriving several exact relations among these quantities and then illustrating them with simple real and computer experiments. I wrote a fairly complete review on the status of the field in 2012 (1) (for more recent complementary reviews, see References 15–21), so the present much shorter review highlights what one could identify as a second phase that we have entered since then. We are now at the stage where we can use these thermodynamic concepts to infer otherwise hidden properties of these systems of which the physical entropy production is arguably the most prominent one. Thermodynamic inference, conceived here rather broadly, was introduced in a more specific sense by Alemany et al. (22) as a strategy to infer hidden physical properties by analyzing experimental data from single-molecule experiments with fluctuation relations assuming essentially Gaussian distributions (see also Reference 23).

After recalling the basic principles of stochastic thermodynamics in Section 2, I focus on the role of coarse graining for entropy production in Section 3, on identifying entropy production for active particles in Section 4, and on the thermodynamic uncertainty relation as a tool for thermodynamic inference in Section 5. In Section 6, I briefly touch on ongoing work concerning ramifications and generalizations of the uncertainty relation.

2. BASIC CONCEPTS

The basic notions of stochastic thermodynamics follow from applying concepts of classical thermodynamics to individual trajectories first in equilibrium and then under nonequilibrium conditions. In this section, starting from scratch, which should make this presentation accessible for

those entering from different fields, I introduce this approach with an emphasis on how these quantities can be inferred from measurements without quantitative knowledge of the underlying interactions. Usually, theoretical work assumes those to be given.

2.1. Mesostates and Their Thermodynamic Potentials

We start with a closed equilibrium system in contact with a heat bath at inverse temperature β . Each microstate ξ has an energy $H(\xi)$, which may, however, not be known explicitly. In principle, free energy, internal energy, and entropy of this system are given by

$$F = -(1/\beta) \ln \sum_{\xi} \exp[-\beta H(\xi)], \quad U = \partial_{\beta}(\beta F), \quad \text{and} \quad S = \beta^2 \partial_{\beta} F = \beta(U - F), \quad 1.$$

respectively. Throughout this review, entropy is dimensionless; i.e., it is given in units of Boltzmann's constant k_B .

Typically, the dynamics of individual microstates, which in aqueous solution should contain all solvent molecules, is neither observable nor really interesting. On a first level of coarse graining, one focuses on observable mesostates $\{I\}$. Those could be the (binned) positions of a few interacting colloidal particles, or distinguishable conformations of one or a few interacting biopolymers or of molecular motors. In any case, each microstate ξ is assumed to belong to one and only one mesostate I , which is denoted by $\xi \in I$. For a simplified specific example to which we repeatedly return to for an illustration of the general concepts, see **Figure 1**, which shows an enzyme interacting with another molecule.

In the course of time, the system visits these mesostates along a trajectory $I(t)$. From such a long equilibrium trajectory, one could extract, in principle, the equilibrium probability $P_I^e = \lim_{T \rightarrow \infty} (1/T) \int_0^T \delta_{I(t)} dt$, where the integrand records the time the trajectory spends in state I up to total time T . Furthermore, given the microscopic model, the probability to find the system in mesostate I is

$$P_I^e = \sum_{\xi \in I} \exp[-\beta(H(\xi) - F)] \equiv \exp[-\beta(F_I - F)], \quad 2.$$

where the last equality defines the free energy F_I of the state I . Consequently, the free energy difference of any two mesostates can be inferred as

$$\Delta_{IJ} F \equiv F_J - F_I = -(1/\beta) \ln[P_J^e/P_I^e] \quad 3.$$

from experimental data of a long equilibrium trajectory.

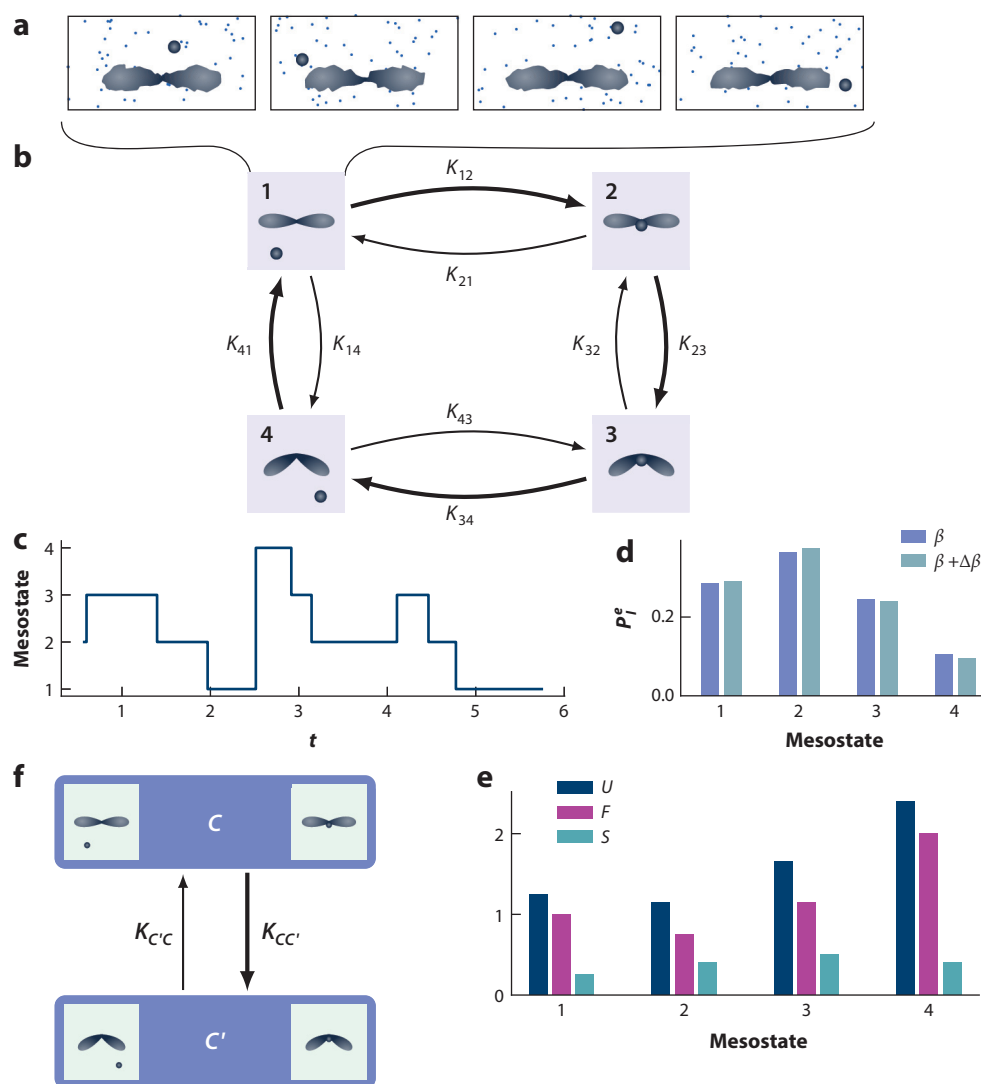
The identification of F_I as free energy is justified by the fact that the internal energy of this mesostate determined from $U_I = \partial_{\beta}(\beta F_I)$ agrees with what one would get from the microscopic model as $U_I = \sum_{\xi \in I} P(\xi|I) H(\xi)$, where

$$P(\xi|I) = \exp\{-\beta[H(\xi) - F]\}/P_I^e = \exp\{-\beta[H(\xi) - F_I]\} \quad 4.$$

is the conditional probability for the microstate ξ given the mesostate I . Finally, the “intrinsic” entropy of mesostate I is given by

$$S_I \equiv \beta^2 \partial_{\beta} F_I = \beta(U_I - F_I) = - \sum_{\xi \in I} P(\xi|I) \ln P(\xi|I), \quad 5.$$

which as the Shannon entropy of the conditional probability indicates roughly how many microstates contribute to the mesostate.

**Figure 1**

Illustrative example of an enzyme interacting with a cofactor molecule embedded in an aqueous solution. (a) Four microstates that differ in the position of the solvent molecules, of the cofactor, and of the atoms making up the enzyme. All these (and many more) microstates are first coarse grained into mesostate 1 characterized by an open conformation of the enzyme and the fact that the cofactor molecule is not bound to it. (b) Mesostates 1, 2, 3, and 4. In mesostate 2, the cofactor is bound to the open enzyme. Mesostates 3 and 4 comprise the closed conformation of the enzyme with and without the cofactor bound to it, respectively. (c) A trajectory $I(t)$, for $t \rightarrow \infty$, leading to the histogram of equilibrium probabilities $\{P_i^e\}$ shown in panel d. From such data taken at (inverse) temperature β and $\beta + \Delta\beta$, the thermodynamic potentials F_I , S_I , and U_I , for $I = 1, 2, 3$, and 4, can be inferred as described in the main text and shown in panel e. Coarse graining on the level of mesostates discussed in Section 3 below is illustrated in panel f, assuming that the cofactor molecule is not observable, which leads to two coarse-grained mesostates $C \equiv \{1, 2\}$ and $C' \equiv \{3, 4\}$.

From an inference point of view, it is crucial to note that free energy differences between such mesostates are not the only quantities that can be extracted from a sufficiently long equilibrium trajectory. Recording such a trajectory at a slightly different temperature gives access to the β -derivative of $\Delta_{IJ}F$. Consequently, by using Equation 5, the difference in intrinsic entropy and internal energy between any two mesostates at fixed temperature are both accessible experimentally as well, and, hence, well defined. Their absolute values are not well defined, but neither are those of the ensemble quantities (Equation 1), at least not in classical systems. I am stressing this point because the concept of trajectory-dependent thermodynamic quantities has recently been questioned fundamentally in an editorially highlighted article (24). The identification of these quantities, which can be derived from a trajectory as shown for the example in **Figure 1**, assumes implicitly weak coupling between the system and heat bath. For a small system, like a biomolecule, the interaction with the solvent, which serves as the heat bath, is not necessarily much smaller than the conformation-dependent, i.e., mesostate-dependent, part of its internal energy. Even in such a strongly coupled case, the thermodynamic potentials can still be identified as shown recently (25–29).

Equilibrium does not have an arrow of time. Hence, the joint probability to observe the system in state I at time t and then in state J at the later time t' is the same as the one for observing it earlier in J and later in I . Introducing conditional probabilities, we thus have

$$P(J, t' | I, t) P_I^e = P(I, t' | J, t) P_J^e. \quad 6.$$

Expanding this relation for small $t' - t$, we get with Equation 3

$$K_{IJ}/K_{JI} = \exp[-\beta \Delta_{IJ}F] = \exp[-\beta \Delta_{IJ}U + \Delta_{IJ}S], \quad 7.$$

where $K_{IJ} \equiv \partial_{t'} P(J, t' | I, t)|_{t'=t}$, which must be independent of t due to time translational invariance in equilibrium.

2.2. Timescale Separation and Master Equation

So far, the identification of the set of mesostates has been arbitrary. Progress toward a thermodynamic structure with a first and second law can be made if the mesostates are such that the dynamics of microstates within each of them is much faster than the dynamics between the mesostates. Under this crucial assumption of a timescale separation, the dynamics between the mesostates become memory-less; i.e., the probability for a transition from a present state I to a future state J is independent of how long the system has already been in state I and how it got there. Specifically, the probability $P_I(t)$ for finding the system in state I at time t then evolves according to the master equation

$$\partial_t P_I(t) = \sum_J [P_J(t) K_{JI} - P_I(t) K_{IJ}]. \quad 8.$$

The $\{K_{IJ}\}$, which thus have become genuine transition rates, are still constrained through Equation 7, which is often called a local detailed balance condition. As important consequences of the master equation dynamics, one can show that (a) the equilibrium distribution (Equation 2) remains invariant; (b) in equilibrium, there is no net flow across any link (IJ), which means that in a long trajectory the number of transitions between I and J is the same as the number of those between J and I ; and (c) any initial distribution $\{P_I^0\}$ will finally approach $\{P_I^e\}$ provided the set of mesostates is connected, i.e., does not split into subsets among which there is no link (30). Furthermore, the timescale separation implies that this dynamics can be applied not only to equilibrium

but also to a relaxation process from an arbitrarily prepared initial distribution $\{P_I^0\}$. In the example introduced in **Figure 1**, such a relaxation process would happen if the system was initially prepared in such a way that the bound mesostates 2 and 3 do not occur, e.g., by initially trapping enzyme and cofactor separately.

2.3. Thermodynamics Along a Trajectory

Along a trajectory $I(t)$, the internal energy of the system becomes a stochastic quantity, $U(t) = U_{I(t)}$. Because the system is closed, any energy change of the system is compensated by a corresponding change in the energy of the heat bath, which can be interpreted as a perpetual exchange of heat along an individual trajectory (7, 8). For a trajectory $I(t)$ starting at time $t = 0$ in state I^0 and ending up at time \mathcal{T} in state $I^\mathcal{T}$, the exchanged heat becomes

$$Q[I(t)] = -(U_{I^\mathcal{T}} - U_{I^0}) = -\Delta U[I(t)], \quad 9.$$

with the sign convention that $Q > 0$ corresponds to heat dissipated in the bath. Because differences in internal energy of mesostates can be inferred from an equilibrium trajectory, the heat exchanged along any trajectory can be inferred as well.

Quite generally, entropy production along a trajectory can be defined as a quantitative measure of a broken time-reversal symmetry (31). In the setting of the closed system discussed so far, such an asymmetry can arise only from a nonequilibrium initial distribution $\{P_I^0\} \neq \{P_I^e\}$. Denoting the “time-reversed” trajectory by $\tilde{I}(t) \equiv I(\mathcal{T} - t)$, the total entropy change along a trajectory can be identified as

$$\Delta S_{\text{tot}}[I(t)] \equiv \ln \left\{ P[I(t)] / \tilde{P}[\tilde{I}(t)] \right\}, \quad 10.$$

where $P[I(t)]$ and $\tilde{P}[\tilde{I}(t)]$ are the probabilities to observe the original and the (fictitious) time-reversed trajectory starting in the given initial and resulting final distribution, respectively (1). Since in equilibrium any trajectory is as probable as its time-reversed partner, this entropy change vanishes identically for any trajectory provided the initial distribution is the equilibrium one. Note that a similar statement does not hold for the dissipated heat in Equation 9. For the master equation dynamics (Equation 8), using the explicit expression for $P[I(t)]$, this entropy change can be further evaluated as a sum of three terms (9, 32),

$$\Delta S_{\text{tot}}[I(t)] = \beta Q[I(t)] + \Delta S[I(t)] + \Delta S_{\text{sto}}[I(t)]. \quad 11.$$

The first term is the conventional entropy change in the heat bath induced by the dissipated heat (Equation 9). The second one $\Delta S[I(t)] \equiv S_{I^\mathcal{T}} - S_{I^0}$ is the change in intrinsic entropy (Equation 5) often tacitly ignored, which, however, is justified only if the mesostates have the same, or an ignorable, internal structure. Finally, the third term is the change in stochastic entropy $S_{\text{sto}}(t) \equiv -\ln P_{I(t)}(t)$. In equilibrium, this last term compensates the changes of intrinsic entropy and the entropy of the heat bath. It can be inferred experimentally by repeatedly drawing trajectories from a given initial distribution. Thus, all three contributions to physical entropy production can be inferred from experimental trajectories provided an ensemble of them can be generated with a prescribed initial condition $\{P_I^e\}$, which could equally well be post.

After averaging over any initial distribution that is strictly positive on all states, the total entropy change obeys the integral fluctuation theorem (IFT) $\langle \exp[-\Delta S_{\text{tot}}] \rangle = 1$ for any \mathcal{T} , from which one gets the second law on the ensemble level as $\langle \Delta S_{\text{tot}} \rangle \geq 0$ (9). This result should not be mistaken for a fundamental proof of the second law, since with the assumption of a timescale separation and

equilibration within each mesostate the crucial ingredients for irreversibility have been put in “by hand” when formulating the master equation.

2.4. Systems in Contact with Particle and Work Reservoirs: Nonequilibrium Steady States

The closed system coupled to a heat bath described so far will ultimately come to equilibrium. For problems involving transport of particles (like electrons), or chemically driven molecular motors working against an external load, reservoirs that provide these particles or the chemical educts at a certain chemical potential must be introduced into this framework. A conceptually clean approach is to imagine a closed supersystem for which the approach just described can be used.

The supersystem contains these reservoirs apart from the system of interest. By splitting the thermodynamic potentials, in particular, the free energy, of the mesostates of the supersystem into those of the system of interest proper, or “core system,” and the reservoirs, one obtains

$$K_{IJ}/K_{JI} = \exp \left[-\beta \left(\Delta_{IJ}F - \sum_{\alpha} d_{IJ}^{\alpha} \mu_{\alpha} + f d_{IJ} \right) \right]. \quad 12.$$

as an extended local detail balance condition for transitions between mesostates of the core system following the relation: The total free energy change of the super system has thus been split into (a) the free energy change of the core system, $\Delta_{IJ}F$, (b) the change in the free energy of the reservoirs that provide (for $d_{IJ}^{\alpha} > 0$) and accept (for $d_{IJ}^{\alpha} < 0$) the d_{IJ}^{α} particles of species α at a chemical potential μ_{α} that are involved in a transition $I \rightarrow J$ of the core system, and (c) putative mechanical work delivered in a mechanical step of length d_{IJ} against an externally imposed force f . The core system has thus become an open system connected to a heat bath with inverse temperature β and chemostats with chemical potentials $\{\mu^{\alpha}\}$ and which is possibly subject to an external force f . For an illustration, see **Figure 2** for a simplified model of a molecular motor and specific values of the quantities showing up in the ratio of rates (12).

For time-independent chemical potentials and external force, the dynamics (Equation 8) will run into a nonequilibrium steady state (NESS) with the stationary probability P_i^s to find the system in state I at any given time. Its specific form for the example of the molecular motor shown in **Figure 2** is given in the caption. The total entropy production associated with a trajectory $I(t)$ as log ratio of the probability to observe the original and the time-reversed trajectory given by Equation 10 then becomes

$$\Delta S_{\text{tot}}[I(t)] = \sum_{IJ} n_{IJ}(\mathcal{T}) \ln(P_i^s K_{IJ}/P_j^s K_{JI}), \quad 13.$$

where $n_{IJ}(\mathcal{T})$ is the number of transitions from I to J in total time \mathcal{T} . The mean rate of entropy production is (33)

$$\sigma = (1/2) \sum_{I < J} (P_i^s K_{IJ} - P_j^s K_{JI}) \ln(P_i^s K_{IJ}/P_j^s K_{JI}) \geq 0. \quad 14.$$

In such a NESS, the probability distribution of total entropy production obeys a detailed FT (9),

$$\ln[p(-\Delta S_{\text{tot}})/p(\Delta S_{\text{tot}})] = -\Delta S_{\text{tot}}, \quad 15.$$

for any arbitrary (but fixed) length \mathcal{T} of trajectories.

For the NESSs described here, it is crucial that the embedding system still provides the ordinary (typically room) temperature. Still, certain variables may then behave as if they were at

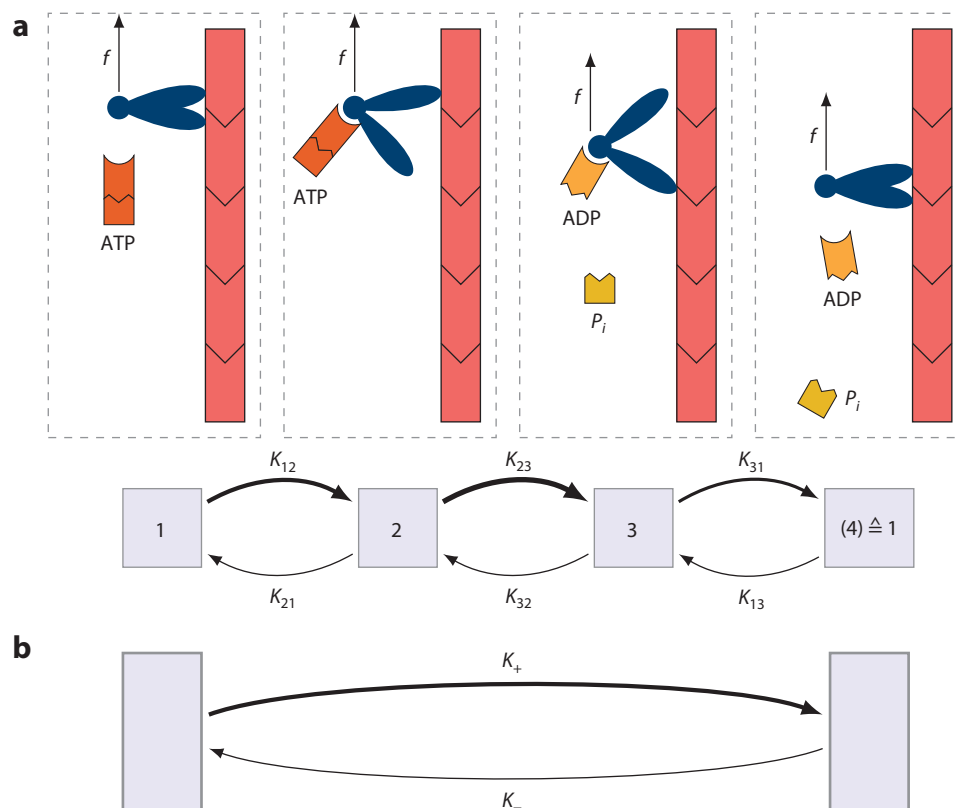


Figure 2

Sketch of a molecular motor with two “heads” stepping along a filamentous track with elementary (or “repeat”) distance d against an externally applied force f . (a) A three-state model. In state 1, an ATP molecule can bind to the motor leading to state 2. Subsequent hydrolysis of ATP to ADP and release of the inorganic phosphate molecule P_i generates a step of the front head leading to state 3. With the release of ADP, the rear head follows. Thus, the cycle of motor conformations has been closed while the motor has advanced one step along the track. Thermodynamic consistency requires that each step can occur backward, however, at typically a much smaller rate. The quantities showing up in the ratio of rates (Equation 12) can be specified as follows: With $\alpha = T, D$, and P denoting the three relevant molecular species, we get $d_{12}^T = 1$, $d_{23}^P = -1$, $d_{31}^D = -1$, $d_{11}^T = -d_{11}^D$, and the other $d_{IJ}^\alpha = 0$. Likewise, for the distance stepped against the force, we have $d_{23} = d_{31} = d/2$, $d_{12} = 0$, and $d_{11} = -d_{11}$. Specifying the $\Delta_{IJ}F$ would require a more detailed model or determining the thermodynamic potentials from a trajectory of the motor under equilibrium conditions, i.e., with $\mu_T = \mu_D + \mu_P$ and $f = 0$ as explained in Figure 1. For a concrete example of a stationary state, we consider the special case of all backward rates being equal, $K_{21} = K_{32} = K_{13} \equiv K_-$, leading to $P_1^s = [K_{23}K_{31} + (K_{31} + K_-)K_-]/N$ and its cyclic permutations for P_2^s and P_3^s . The normalization N follows from $P_1^s + P_2^s + P_3^s = 1$. (b) Further coarse graining leading to a minimal model with just a forward rate K_+ and a backward rate K_- used when introducing the thermodynamic uncertainty relation in Section 5 below. Abbreviations: ADP, adenosine diphosphate; ATP, adenosine triphosphate.

an effective, higher, temperature caused by the driving (34). In a recent joint experimental and theoretical study, this effect was systematically explored for a colloidal particle and for DNA hairpins driven by stochastically oscillating laser traps (35). This study revealed that there are typically parameter ranges in which an effective temperature can be meaningfully identified from a fluctuation-dissipation theorem, whereas in others correlation and response function do not

simply become proportional. As a rule of thumb, if the driving decorrelates faster than relevant intrinsic relaxation times of the system, the concept of an effective temperature is a sensible one. A different issue is the response of such a steady state to a small physical temperature change, for which an elegant response theory has been developed recently (36).

3. COARSE GRAINING IN A NONEQUILIBRIUM STEADY STATE AND ITS EFFECT ON ENTROPY PRODUCTION

A crucial assumption of stochastic thermodynamics is that all relevant mesostates are observed and that the underlying fast hidden dynamics on the microstate level is equilibrated (1, 37). If not all relevant mesostates are experimentally accessible, a trajectory on a coarser level will no longer follow Markovian dynamics. Consequently, residence times of the observable states will no longer be exponentially distributed. What can still be inferred about entropy production?

3.1. Entropy Production from Time Reversal

On a general level, coarse graining loses parts of the genuine physical entropy production. We define coarse graining by a many-to-one mapping that associates with each (mesoscopic) trajectory $I(t)$ uniquely a coarse-grained one $C(\tau)$. If both descriptions contain continuous time, the time arguments agree, i.e., $\tau = t$. However, the finite temporal resolution in experiments may require that the coarse-grained data are taken at discrete times $\tau \in \{t_i\}$ only, which is an admissible variant of coarse graining. In any case, the expression given in Equation 10 offers a first option to identify a coarse-grained entropy production rate since the log ratio of these probabilities is still well defined and experimentally, in principle, retrievable, even though generating sufficient statistics might be nontrivial. This coarse-grained entropy production then provides a lower bound on the true one according to

$$\begin{aligned} \langle \Delta S_{\text{cgr}}[C] \rangle &\equiv \sum_C p(C) \ln[p(C)/p(\tilde{C})] = \sum_{C,I} p(C|I)p(I) \ln \frac{\sum_I p(C|I)p(I)}{\sum_{\tilde{I}} p(\tilde{C}|\tilde{I})p(\tilde{I})} \leq \\ &\sum_{C,I} p(C|I)p(I) \ln \frac{p(C|I)p(I)}{p(\tilde{C}|\tilde{I})p(\tilde{I})} = \sum_{C,I} p(C|I)p(I) \left[\ln \frac{p(C|I)}{p(\tilde{C}|\tilde{I})} + \ln \frac{p(I)}{p(\tilde{I})} \right] = \langle \Delta S_{\text{tot}}[I] \rangle. \end{aligned} \quad 16.$$

Here, C and I are short for the whole trajectories $C(\tau)$ and $I(t)$, respectively. For the inequality, one needs the log-sum inequality, $\sum_i a_i \ln[\sum_i a_i / \sum_i b_i] \leq \sum_i a_i \ln[a_i / b_i]$ (valid for any $a_i \geq 0$ and $b_i \geq 0$), and for the final step $p(C|I) = p(\tilde{C}|\tilde{I}) = 1$ or 0 , depending on whether I is contained in C or not. This reasoning, well established in information theory (38), has been introduced to stochastic thermodynamics first in the context of time-dependent-driven systems (39–42) and then transferred to NESSs (43).

In general, one cannot expect that this lower bound retrieves the full entropy production. It does so only in special cases, e.g., when the hidden degrees of freedom are indeed in an equilibrium constrained to the instantaneous values of the observable ones. The quality of this lower bound has been assessed in model calculations for a discrete ratchet by Roldan & Parrondo (44, 45) and for a chemical network by Muy and coworkers (46).

Remarkably, ΔS_{cgr} as log ratio of corresponding probabilities obeys the detailed FT (Equation 15). Therefore, an experimentally observed “validity” of an FT for such a variable would not imply a physically complete identification of genuine entropy production. Kawaguchi



& Nakayama have derived conditions under which the missing entropy, $\Delta S_{\text{tot}} - \Delta S_{\text{cgr}}$, obeys an integral fluctuation relation (47). While finding such relations is theoretically interesting, they are of limited value from an experimental perspective as this quantity, by definition, can neither be observed nor inferred.

3.2. Mapping to a Markov Model

A second strategy to infer entropy production is by mapping the coarse-grained system to effectively Markovian dynamics on the set of the observable mesostates $\{C, C', C'', \dots\}$, for which **Figure 1f** gives an example. Because such a procedure is not unique, conditions on the choice of coarse-grained transition rates must be imposed. It is natural to require dynamic consistency, which means that the Markov model should reproduce both the stationary probabilities on the coarse-grained level $\{P_C^s\}$ and the observed mean number of transition $\langle n_{CC'} \rangle$ between any directed pair of states $C \rightarrow C'$. These conditions imply that the rates must be chosen as $K_{CC'} = \langle n_{CC'} \rangle / P_C^s \mathcal{T}$. Then the experimentally inferred, “apparent,” entropy production along a trajectory becomes

$$\Delta S_{\text{app}}[C(t)] = \sum_{CC'} n_{CC'} \ln[P_C^s K_{CC'} / P_{C'}^s K_{C'C}] + \Delta S_{\text{sto}}[C(t)]. \quad 17.$$

In general, this apparent entropy production does not fulfill a detailed FT (Equation 15) because the observed weight of a coarse-grained trajectory does not correspond to the weight that would be generated for the same trajectory by the Markovian dynamics with the rates $\{K_{CC'}\}$.

An experimental study with two paramagnetic colloidal particles, each driven along a periodic potential found the approximative validity of a modified FT, with an additional factor on the right-hand-side of Equation 15, for the apparent entropy production resulting from observing only one particle (48). This surprising finding was recently rationalized as a lack of statistics of extreme fluctuations and a “fine-structure” that appeared generically in motion along periodic potentials (49, 50). From a general perspective, even more significant is the finding that the tails of the probability distribution of the apparent entropy production (Equation 17) always obey such a modified FT in the limit of long observation times. Otherwise inaccessible properties can be inferred with some additional information on the microscopic structure of the system, like in this case the true entropy produced in one rotation of the visible degree of freedom (50). Another strategy to preserve the entropy production under coarse graining has been employed by Knoch & Speck via coarse-graining cycles (51).

3.3. Further Approaches

For certain classes of systems with relevant unobserved degrees of freedom, alternative approaches have been developed.

3.3.1. Systems with timescale separation. If the dynamics within each mesostate is fast, whereas transitions between the coarse-grained mesostates are slow, the effective coarse-grained dynamics is still Markovian. However, this does not imply that if entropy production is determined according to Equation 13, the full entropy production is recovered. Only if the fast dynamics does not contain closed cycles that lead to entropy production, then timescale separation allows one to infer the full entropy production from the coarse-grained one (52). Otherwise, an “anomalous” entropy production occurs that survives even under infinite timescale separation (53). A somewhat different scheme was developed earlier by Rahav & Jarzynski (54). Wang and coworkers have recently shown that in discrete systems with timescale separation the entropy production associated

with the slow degrees of freedom can also be inferred from a violation of the fluctuation-response relation (55); this was done by generalizing an earlier result for continuous degrees of freedom by Harada & Sasa (56).

3.3.2. Bipartite and masked dynamics. A slightly different class of coarse graining assumes that only a selected set of transitions is observable. In the important class of bipartite systems, each state contains two labels (57). In the observable transitions the first one changes (keeping the second one the same), whereas in the hidden (or “masked”) transitions the second one changes while the first remains fixed. The true total entropy production can then be split into one being caused by the observable transitions and one being caused by the hidden or masked states. Various IFTs and inequalities between these quantities have been proven and illustrated for model systems (57, 58). The main problem with employing this framework on experimental systems is that without knowing both labels the mere observation of the coarse-grained trajectories will not suffice to extract the quantities that are necessary to infer the entropy production due to the observable transitions let alone those associated with the hidden ones.

The same caveat holds for a related class of systems lacking a bipartite structure where one, or several, transitions are identified as observable and the remaining ones are identified as hidden. Theoretically, criteria for IFTs and inequalities can be proven, but their experimental significance for inferring thermodynamic quantities remains open at this stage (59, 60).

3.3.3. Molecular motors. For a large class of molecular motor models with attached probe particles to which external loads can be applied, coarse graining over the probe particle can be performed in such a way that the mean apparent entropy production of the coarse-grained model corresponds to the full entropy production (61). In this approach, the rates $\{K_{CC'}\}$ are chosen such that the mean currents $\langle n_{CC'} - n_{C'C} \rangle / \mathcal{T}$ are reproduced (but not the individual mean number of transitions from C to C' and vice versa). In addition, a local detailed balance condition on the level of the coarse-grained states could be imposed. However, this approach rests crucially on the fact that the effective one-dimensional motion of the probe particle cannot generate cycles with entropy production.

4. ACTIVE PARTICLES

Active particles have become a major paradigm in statistical physics, as covered by several recent reviews (see References 62–73). An investigation of the associated entropy production, on which we focus here, has, however, just been started.

4.1. Models

Active particles possess a propulsion mechanism that leads to an active velocity \mathbf{u} with speed $u \equiv |\mathbf{u}|$ along an intrinsic director \mathbf{n} . In the presence of an external potential and/or interactions with other particles, the equation of motion for the position \mathbf{r} reads as

$$\partial_t \mathbf{r} = -\mu \nabla V + \mathbf{u} \quad 18.$$

in the overdamped limit, which is appropriate for most particles in aqueous solution. Here, μ is a mobility, i.e., an inverse friction coefficient, and V the total potential acting on the active particle. Following several previous works, there is no noise yet in this equation of motion. For notational simplicity, we deal here with a single active particle. For an interacting collection of

them, quantities like $u, \mathbf{r}, \mathbf{n}, V$, and so on, would get a particle index. All statements made here and in the following hold true for this interacting case as well.

At least three different classes of active particles can be distinguished by the dynamics of \mathbf{u} . (a) For run-and-tumble particles (RTPs), the speed u is constant. A run-mode with constant director is followed by a tumble event, in which the director changes randomly to a new direction. (b) Active Brownian particles (ABPs) are characterized by a constant speed u and rotational diffusion of the director. (c) Finally, for active Ornstein–Uhlenbeck particles (AOUPs), both speed and director change according to the Langevin equation,

$$\partial_t \mathbf{u} = -\mathbf{u}/\tau + [2\bar{u}^2/\tau]^{1/2} \boldsymbol{\eta}, \quad 19.$$

with $\boldsymbol{\eta}(t)$ as standard white noise. Here, τ is the relaxation time of the propulsion velocity, and \bar{u}^2 its mean square.

On the ensemble level, for all three classes, the dynamics will reach a steady state provided the motion remains bounded either due to a confining potential or a confining geometry. Furthermore, without noise in Equation 18, the trajectory of the velocity $\mathbf{u}(t)$ determines the spatial trajectory $\mathbf{r}(t)$ completely. Even though generating the propulsion requires driving as further discussed below, the dynamics proper of the self-propulsion $\mathbf{u}(t)$, as characterized above, is not only independent of the spatial degree of freedom but resembles formally nondriven dynamics. Consequently, the distribution $P^s(\mathbf{u})$ is of an equilibrium type, which, in the absence of any orienting field for the director, is uniform for RTPs and ABPs and a Gaussian for AOUPs.

4.2. Entropy Production

If one wanted to identify entropy production for any of these classes using Equation 10 by comparing the weight of a forward trajectory $\mathbf{u}(t)$ with that of a time-reversed one $\tilde{\mathbf{u}}(t)$, one has formally two options. Either one keeps the original orientation, $\tilde{\mathbf{u}}(t) = \mathbf{u}(\mathcal{T} - t)$, or one reverses it, $\tilde{\mathbf{u}}(t) = -\mathbf{u}(\mathcal{T} - t)$. In the absence of a potential (and interactions in the many-particle case), the latter choice corresponds to what one would naively call time reversal, since it leads in position space to $\tilde{\mathbf{r}}(t) = \mathbf{r}(\mathcal{T} - t)$. Crucially, since the orientation \mathbf{u} dynamics is effectively in equilibrium, $p[\tilde{\mathbf{u}}(t)]/p[\mathbf{u}(t)] = 1$ for both choices, and thus entropy production according to Equation 10 vanishes identically along each trajectory and, hence, also in the mean.

For AOUPs, arguments based on time-reversal have led to a different result. The equations of motion (Equations 18 and 19) can formally be mapped to effectively underdamped dynamics with a velocity dependent force (74). This mapping allows a perturbative approach to the stationary distribution for a small relaxation time τ leading to insights into the occurrence of phenomena like motility-induced phase separation and the like. However, if one tries to infer entropy production from these effective underdamped dynamics, one obtains an expression that vanishes for harmonic interactions (74). Again, there is a second option for how to perform the time reversal, which corresponds effectively to keeping the orientation of the director, leading to nonvanishing entropy production for harmonic interactions (75).

These conflicting results, depending on how and on which level time-reversal is applied, point to a deeper problem. A further hint that something fundamental is not quite captured by the argument given in the above two paragraphs follows from the naive observation that in all approaches a single free self-propelled particle would not lead to entropy production at all. By contrast, such a motion necessarily causes viscous stresses in the surrounding fluid with viscosity η for which one would expect a contribution $\sim \eta \langle u^2 \rangle$ to the overall entropy production rate.

The problem is that the starting equation, Equation 18, is thermodynamically inconsistent on two grounds. First, the presence of a friction term in an equation of motion like Equation 18 requires that the corresponding noise is included as well. If the mobility μ is supposed to be the Stokes' one, i.e., $\mu = 1/6\pi R\eta$ for a spherical particle of radius R , a thermal noise term with correlations $\langle \zeta(t)\zeta(t') \rangle = 2(\mu/\beta)\delta(t-t')$ must be added to the right-hand side of Equation 18. Second, and even more important, any self-propulsion ultimately based on physicochemical processes occurs in a finite temperature environment. Hence, it comes necessarily with its own noise that acts along the instantaneous director $\mathbf{n}(t)$. Modeling this noise as white with correlations $\langle \zeta_{ac}(t)\zeta_{ac}(t') \rangle = 2(\mu_{ac}/\beta)\delta(t-t')$, one finally gets an augmented Langevin equation,

$$\partial_t \mathbf{r} = -[\mu + \mu_{ac}\mathbf{n} \otimes \mathbf{n}]\nabla V + u\mathbf{n} + \boldsymbol{\zeta} + \zeta_{ac}\mathbf{n}. \quad 20.$$

Even though the active mobility, μ_{ac} , with its inverse being an active friction, arises from the noise in the chemical reactions, it is affected by the hydrodynamics. An explicit calculation of this mobility for a Janus particle would require solving the corresponding hydrodynamic problem (76, 77). It is conceptually crucial, however not yet universally recognized, that this active mobility is not the Stokes' one because the latter is related to the translational noise exerted by the surrounding fluid.

The Langevin Equation 20 has first been derived as the continuum limit of a thermodynamically consistent minimal lattice model for ABPs (78). This derivation shows explicitly why the active noise leads to a corresponding active mobility, caused by active friction in front of the potential term: If the propulsion mechanism must act against a potential force, the corresponding reaction occurs with a slightly diminished rate. Such a coupling between translation and chemical reactions has also been found in a linear response treatment (79). From a stochastic thermodynamics perspective, the Langevin Equation 20 without the active terms has been analyzed by Speck (80), and its underdamped version by Chaudhuri (81, 82). A thermodynamic perspective on the overdamped AOUP version (again without recognizing the role of active noise and mobility) was given by Szamel (83) and for the original AOUP model (Equations 18 and 19) by Speck (84) and by Puglisi & Marconi (85).

The mean entropy production rate in the lattice model leading to Equation 20 becomes

$$\sigma_{\text{tot}} = (\beta/\mu_{ac})u^2 - u(\mathbf{n}\nabla V) \quad 21.$$

in the continuum limit (78). Without a potential, only the first term contributes, which indeed is of the form that one would expect naively. Even in the presence of a potential, the translational mobility μ_{ac} does not show up explicitly in this second term. However, the corresponding terms will affect the stationary distribution $P(\mathbf{r}, \mathbf{n})$ and hence the second contribution in Equation 21. The lattice model introduced in Reference 78 has a constant propulsion speed and thus provides a thermodynamically consistent model for ABPs. Thermodynamically consistent models for AOUPs could be developed along similar lines using several chemical reaction channels with each leading to a different propulsion speed.

Crucially, in general, the physical entropy production Equation 21 cannot be recovered by applying the expression Equation 10 for either version of time reversal, $\tilde{\mathbf{n}}(t) \equiv \mathbf{n}(\mathcal{T}-t)$ and $\mathbf{n}(t) = -\mathbf{n}(\mathcal{T}-t)$, to the Langevin dynamics (Equation 20). The first variant succeeds only if translational mobility (and noise) is set to zero; the second variant never succeeds (78). This failure occurs because the Langevin Equation 20 refers to position only, whereas information about the reaction has been lost; i.e., it has effectively been coarse-grained away: An increment along the director could arise from either a chemical reaction with its inevitable dissipation or an ordinary thermal noise, which, in the absence of a potential, does not cause dissipation. Without explicitly

keeping a chemical coordinate, modeled, e.g., through additional Langevin dynamics as suggested in Reference 73, these two alternatives cannot be distinguished. The lesson to be taken from this discussion is that without additional knowledge of the underlying microscopic events, entropy production cannot be uniquely inferred from trajectory data for the position only.

4.3. Colloidal Particles in Active Baths

So far, we have described active particles as a nonequilibrium system embedded in an aqueous solution that serves both as thermal bath with a well-defined temperature and as reservoir for molecules with well-defined chemical potentials that are involved in the reactions generating the self-propulsion. A further class of systems emerges if one or several passive colloidal particles are added to such a suspension. Two complementary perspectives on such a system are conceivable.

First, one can describe the mixture of active and passive particles by a set of Langevin equations of the type given in Equation 20 where for the passive particles active mobilities and noise are deleted (78). Such an approach does not pose any conceptual problems and stays well within the realm of stochastic thermodynamics. Second, one could invoke the idea of a nonequilibrium bath, which, taken at face value, may sound like a *contradictio in se* since in thermodynamics a bath or reservoir is a genuine equilibrium system. One limiting case for which such a parlance can hardly be criticized are systems in which the active forces, e.g., generated by active particles hitting a passive one, have a correlation time that is small compared with relaxation times of the (passive) system of interest. In a Langevin description, the corresponding dynamics of the passive particle then basically experience stronger thermal forces which correspond to a higher effective temperature of this nonequilibrium bath.

An experimentally realizable version of an active bath is suspensions of bacteria for which anomalous diffusion (86), active stress fluctuations (87), and an effective temperature (88) have been measured. In the experiment reported in Reference 89, a colloidal particle in a time-dependent harmonic potential has been used to demonstrate the, not surprising, failure of the Jarzynski and Crooks relations with such an active bath. Interestingly, these authors could restore these FTs using an effective potential derived from the stationary distribution.

In another intriguing experiment, such a system has been used to implement a Brownian heat engine coupled to an active bath (90). For two equilibrium baths with a hot and cold temperature, T_h and T_c , such a setup was introduced in 2007 theoretically in Reference 91 as a paradigm for studying efficiency, and efficiency at maximum power, on a micron scale for a Carnot cycle. In the Stirling version, this suggestion was implemented a few years later in the lab by Blickle & Bechinger (92), in which the hotter heat bath was generated by additional local heating, leading to a typical ratio of $T_c/T_h \simeq 0.8$. In a recent experiment (90), the activity of the bacteria leads to a substantially higher effective temperature and a correspondingly larger effective efficiency. This very experiment, however, also points to the limitations of this perspective since the distribution of the passive particle in the harmonic trap turned out to be distinctly non-Gaussian, which prevents a unique identification of a suitable effective temperature of this nonequilibrium bath (93).

An interesting approach that could ultimately lead to a systematic theory of such nonequilibrium baths has been suggested by Steffenoni et al. (94). A weak coupling assumption between active and passive particles allows them to first consider perturbatively the effect the passive ones impose on the genuine active NESS. In a second step, they can then derive generalized Langevin equations with memory for the passive particles. Because the noise in these Langevin equations is not correlated with the memory in the friction, the active particles are thus manifestly embedded in a nonequilibrium bath. Whether and how this approach can be extended to strongly interacting systems remains to be seen.

5. THERMODYNAMIC UNCERTAINTY RELATION

5.1. Formulation

The basic idea behind the thermodynamic uncertainty relation can be introduced with the arguably simplest nonequilibrium process. This is an asymmetric random walk, in which a particle symbolizing, e.g., the position of a molecular motor on a track, moves with a rate K_+ to the right and with a smaller rate K_- to the left, which represents also a coarse-grained version of the motor model discussed in **Figure 2b**. After a time \mathcal{T} , the average position is $\langle n \rangle = j^s \mathcal{T}$, with the stationary, or mean, current $j^s = K_+ - K_-$. The typical fluctuations are encoded in the dispersion, or diffusion, coefficient $D \equiv \langle (n - \langle n \rangle)^2 \rangle / 2\mathcal{T} = (K_+ + K_-)/2$. This ubiquitous model becomes thermodynamically consistent when we appreciate that the breaking of time-reversal symmetry, $K_+ \neq K_-$, necessarily requires nonequilibrium conditions that lead to free energy consumption. In fact, the entropy production rate associated with this process follows from Equation 14 as $\sigma = (K_+ - K_-) \ln[K_+/K_-]$ since there is effectively only one mesostate. A trivial calculation then shows that the three fundamental quantities, j^s , D , and σ , just given obey the relation

$$\sigma \geq j^{s2}/D. \quad 22.$$

Thus, at a given current, small dispersion requires a minimal dissipation rate. This bound is saturated close to equilibrium, $K_+/K_- \rightarrow 1$.

The surprising fact is that this relation holds with the mean and the dispersions of any current that can be deduced from Markovian dynamics on a discrete set of states as first conjectured in Reference 95 based on extensive numerical and analytical work. An elegant rigorous proof using large deviation techniques was then found in Reference 96. This universally valid relation thus allows one to infer a lower bound on the entropy production rate σ in any such network by measuring any of its currents and the corresponding dispersion. More precisely, monitoring $X(\mathcal{T}) = \sum_{IJ} d_{IJ} n_{IJ}(\mathcal{T})$, where $d_{IJ} = -d_{JI}$ is any antisymmetric increment associated with a transition $I \rightarrow J$, yields

$$j^s \equiv \langle X(\mathcal{T}) \rangle / \mathcal{T} \quad \text{and} \quad D \equiv \lim_{\mathcal{T} \rightarrow \infty} [\langle X^2(\mathcal{T}) \rangle - \langle X(\mathcal{T}) \rangle^2] / 2\mathcal{T} \quad 23.$$

that can be used in Equation 22.

5.2. Cost of Precision

The inequality, Equation 22, has been dubbed the thermodynamic uncertainty relation, because, in a related interpretation, it shows that the uncertainty of a process and its cost are complementary quantities. We can interpret the system described above as a process that generates a product, here steps, on average linearly in time. The outcome after a fixed time is not sharp but comes with a certain variance. The uncertainty of the process defined as $\epsilon^2 \equiv \langle (n - \langle n \rangle)^2 \rangle / \langle n \rangle^2$ becomes smaller the longer the process runs. Since the thermodynamic cost $C \equiv (\sigma/\beta)\mathcal{T}$ increases linearly with time, the uncertainty relation (Equation 22) implies that

$$C \geq 2/\beta\epsilon^2. \quad 24.$$

Thus, precision, i.e., a small uncertainty, has a minimal cost independent of the duration of the process. If one arranges the steps in a circular fashion as the marks on the face of a clock, Equation 24 gives the minimal cost of such a “Brownian clock” (97). However ingeniously such a clock may be constructed, it will not be able to beat this fundamental bound as long as it operates in a steady state at (inverse) temperature β .

5.3. Inferring Bounds on the Thermodynamic Efficiency of Motors

This thermodynamic uncertainty relation can serve as a powerful technique for deriving upper bounds on the efficiency of molecular machines or motors. Molecular motors, whether biological or artificially built, typically operate in an environment of constant (inverse) temperature β as given by the surrounding aqueous solution. In a steady state, such motors are driven by some chemical input power, P^{in} . They deliver output power $P^{\text{out}} = fv$ against an applied force f at a velocity v . Fluctuations around this average velocity can be characterized by the diffusion coefficient D . The input power is the rate of free energy change of the particle reservoirs providing the educts and accepting the products of the powering chemical reaction. In the simplest case of ATP-hydrolysis, it is the free energy difference associated with this reaction multiplied with the rate of reaction. While the former quantity can be inferred in principle if one knows the concentration of all involved chemicals, inferring the rate of reaction requires assumptions about how the chemical steps are related to the visible mechanical ones.

In contrast, the thermodynamic uncertainty relation yields a bound on the efficiency without invoking any model as follows. First, the mean total entropy production is given by the difference between mean input and output power, $\sigma = \beta(P^{\text{in}} - P^{\text{out}})$. With Equation 22, and choosing the output power $P^{\text{out}} = fv$ as current, the efficiency can be written as (98)

$$\eta = \frac{P^{\text{out}}}{P^{\text{in}}} = \frac{P^{\text{out}}}{P^{\text{out}} + \sigma/\beta} = \frac{vf}{vf + \sigma/\beta} \leq \frac{1}{1 + v/(Df\beta)}. \quad 25.$$

This bound involves with v , D , and f only experimentally accessible quantities. Neither knowledge of the underlying network, i.e., of the specific reaction scheme, is necessary nor does the free energy difference $\Delta\mu$ associated with the ATP hydrolysis enter. In Reference 99, this bound is evaluated using experimental data for a kinesin motor reported in Reference 100. For a related application of the uncertainty relation to molecular motor data, see Reference 101.

For stochastic heat engines, the thermodynamic uncertainty relation can be used along similar lines to prove that with approaching Carnot efficiency the output power must vanish at least linearly except if power fluctuations diverge. This general result clarifies and unifies several recent studies with partially conflicting results (102).

6. GENERALIZATIONS AND RAMIFICATIONS OF THE UNCERTAINTY RELATION

6.1. Finite-Time Uncertainty Relation

The diffusion coefficient D entering the uncertainty relation involves a long-time limit $\mathcal{T} \rightarrow \infty$ in Equation 23. In particular, from an experimental perspective, it would be valuable if it could be replaced by a finite-time expression $D(\mathcal{T})$. Indeed, as conjectured and illustrated with experimental data for a colloidal particle in a stochastically displaced harmonic potential in Reference 103, the uncertainty relation holds even for finite \mathcal{T} , which was proven in full generality in Reference 104.

6.2. Bound on the Large Deviation Function

The uncertainty relation yields a bound on the second cumulant of a current. Surprisingly, the full spectrum of fluctuations as described by a large deviation function can likewise be bounded universally. Specifically, in the long-time limit, the probability to observe the fluctuating current

$j \equiv X(T)/T$ can be written as

$$p(j, T) \sim \exp[-TI(j)], \quad 26.$$

where the rate, or large deviation, function $I(j)$, with $I(j^s) = 0$, determines how the probability of fluctuations away from the mean j^s becomes exponentially small for long observation times. As conjectured in Reference 105 and proven in References 96 and 106, this rate function can be bounded by a quadratic function, the curvature of which is determined by the entropy production rate as

$$I(j) \leq \sigma(j/j^s - 1)^2/4. \quad 27.$$

The uncertainty relation (Equation 22) is a direct consequence of this more general result since $D = 1/[2I''(j^s)]$.

6.3. Bounds for Inference Requiring Additional Input

One appeal of the uncertainty relation is that it bounds the fluctuations of any current by the overall entropy production σ independently of both the specific physical mechanism that drives the process and the topology of the underlying network. If, however, information about these aspects is available, or sought for, stronger bounds can be proven (107, 108). As a paradigmatic one, we consider the topology-dependent and affinity-dependent bound (107),

$$C\epsilon^2 = 2\sigma D/j^{s2} \geq (A/N)^* \coth[A/N]^*/2 \geq \max[2, (A/N)^*]. \quad 28.$$

For each closed cycle in the underlying network, one must form the ratio between its affinity A , which is the entropy production associated with this cycle (33), and its number of states N . The smallest strictly positive value of this ratio among all cycles, $(A/N)^*$, enters this bound. For a unicyclic network of N states, the first inequality is saturated if all forward rates are identical as are all backward rates. In multicyclic networks, the cycle with the smallest A/N potentially leads to the smallest fluctuations and, thus, provides a lower bound on the overall fluctuations.

As one application for thermodynamic inference, consider biochemical or enzymatic networks in which the source of free energy arises from the hydrolysis of ATP. The affinity of any cycle is then given by $A = n\Delta\mu$, where n is the number of ATP molecules consumed in this cycle and $\Delta\mu$ the free energy of the hydrolysis. If the latter is known, measuring the Fano factor of the reaction leads, with Equation 28, to bounds on the minimum number of mesostates involved in the reaction, as discussed in Reference 109.

6.4. Continuous Degrees of Freedom

The uncertainty relation in the original set-up of Markovian dynamics on a discrete set of states can easily be extended to continuous systems that follow an overdamped Langevin equation in steady state (106, 108, 110) and for finite-time and under relaxation (111). In contrast, the extension to a system described by an underdamped Langevin equation is nontrivial because for the latter there is no obvious discretization that maps it to the master equation dynamics (Equation 8) while preserving the entropy production. A recent numerical case study, however, indicates that the uncertainty relation may hold for underdamped systems as well (112). For a general claim in this direction, see Reference 113. For ballistic transport of noninteracting particles between reservoirs of different chemical potential and temperature the uncertainty relation has been shown to hold as well (114). In this case, dissipation takes place only in the reservoirs that thermalize the

transported particles. Intriguingly, the same study also showed that for transport of charged particles in a magnetic field, which breaks time-reversal symmetry, the uncertainty relation holds with a constant $\simeq 0.896$, replacing the factor 2 in Equation 24.

6.5. Time-Dependent Driving

The uncertainty relation applies to a NESS. In general, it does not hold if the driving is time dependent for which arbitrary precision can be reached at a finite cost as first observed in an example of a periodically driven Brownian clock (97). The physical reason for this loophole is the option to effectively confine a particle between moving boundaries in a way that suppresses fluctuations at a moderate cost of driving. It must, however, be appreciated that such time-dependent control of a system involves an additional cost that is usually neglected. If this time-dependent control is included in a thermodynamically consistent manner (115; see also Reference 116), the thermodynamic uncertainty relation is recovered.

For the special case of time-symmetric periodic driving with period Δt , a generalization of the thermodynamic uncertainty relation holds true in the form,

$$\bar{j}^2/D \leq (\exp \Delta S - 1)/\Delta t, \quad 29.$$

where ΔS is the mean entropy production in one period (117). This version of the uncertainty relation was derived for a Markov chain for discrete time with a timestep Δt for which it was noticed earlier that the original version, Equation 22, does not hold (118). The reason is that in the original time-continuous case the variability of the time intervals between jumps leads to larger fluctuations. Because constant driving corresponds to a degenerate case of time-symmetric driving, the result (Equation 29) implies the uncertainty relation for a NESS (Equation 22) through the limit $\Delta t \rightarrow 0$ and $\Delta S = \sigma \Delta t$. A mapping between time-continuous and discrete-time dynamics can be exploited to derive a strengthened version of the uncertainty relation (119). Whether and how mappings between periodically driven systems and NESSs can be used to derive bounds for the periodic case remains to be explored (97, 120–124). Within linear response, a generalized form of the uncertainty relation for time-asymmetric driving has been derived in Reference 125.

6.6. Other Variables and Statistics of Extrema

We have focused on variables associated with currents since the presence of currents is the main feature that distinguishes a NESS from equilibrium. The techniques developed for deriving bounds on current fluctuations can easily be transferred to other variables like the time spent in a state or the activity, also called traffic or frenesy, that counts the total number of transitions between any pair of states irrespective of the direction (113, 126, 127).

In most of the studies mentioned so far, the fluctuations are evaluated up to a fixed final time \mathcal{T} . In a complementary approach, related results can be derived for the fluctuations of a first-passage time, i.e., for the time at which a certain value of a current or another variable is reached for the first time (128, 129). Likewise, the statistics of extreme values of entropy production and other currents show a remarkable universality (130–132).

7. CONCLUDING REMARKS

Entropy production is arguably the most characteristic feature of nonequilibrium systems. Within the framework of stochastic thermodynamics, entropy production can be identified uniquely for

a large class of them. Whether it also can be measured depends on both the resolution of an experiment and knowledge of further crucial parameters of the system under investigation. In this brief review, I have focused on a selection of recent advances that allows inference of this quantity, typically in the form of bounds, under less favorable conditions with incomplete data or knowledge. The discussion of coarse graining has highlighted the subtle role hidden degrees of freedom can have. For active particles, the apparently straightforward strategy of investigating the system under time reversal can be misleading if applied on too coarse a level. The most versatile approach to thermodynamic inference at present seems to be the thermodynamic uncertainty relation and its ongoing generalizations and ramifications that bound entropy production through measurable fluctuations of arbitrary currents.

In closing, I want to mention a few related exciting developments in which, with the tools of stochastic thermodynamics, the thermodynamic cost of driven systems can be assessed and, thus, their efficiency be evaluated. Recently, such an approach has been applied to learning with neural networks (133, 134); to sensory systems (135–142); to biochemical and biophysical networks (143–147), in particular to the cost of precision in oscillating ones (148, 149); and to self-assembly (150). Finally, though quantum systems without coherence are straightforwardly included in the established master equation approach recalled here, a new situation arises whenever coherence and entanglement play a decisive role. It will be interesting to see whether and when stochastic quantum thermodynamics will reach the conceptual maturity and the potential for thermodynamic inference that we have achieved in the classical case covered here.

DISCLOSURE STATEMENT

The authors are not aware of any affiliations, memberships, funding, or financial holdings that might be perceived as affecting the objectivity of this review.

ACKNOWLEDGMENTS

For enjoyable collaboration on some of the more recent topics reviewed here, I would like to thank A.C. Barato and P. Pietzonka. Their comments on this manuscript are gratefully acknowledged as are those by L. Fischer and M. Uhl, whom I also thank for preparing the figures.

LITERATURE CITED

1. Seifert U. 2012. *Rep. Prog. Phys.* 75:126001
2. Pekola JP. 2015. *Nat. Phys.* 11:118
3. Jarzynski C. 1997. *Phys. Rev. Lett.* 78:2690
4. Crooks GE. 1999. *Phys. Rev. E* 60:2721
5. Crooks GE. 2000. *Phys. Rev. E* 61:2361
6. Jarzynski C. 2011. *Annu. Rev. Condens. Matter Phys.* 2:329
7. Sekimoto K. 1997. *J. Phys. Soc. Jpn.* 66:1234
8. Sekimoto K. 1998. *Prog. Theor. Phys. Supp.* 130:17
9. Seifert U. 2005. *Phys. Rev. Lett.* 95:040602
10. Evans DJ, Cohen EGD, Morriss GP. 1993. *Phys. Rev. Lett.* 71:2401
11. Evans DJ, Searles DJ. 1994. *Phys. Rev. E* 50:1645
12. Gallavotti G, Cohen EGD. 1995. *Phys. Rev. Lett.* 74:2694
13. Kurchan J. 1998. *J. Phys. A: Math. Gen.* 31:3719
14. Lebowitz JL, Spohn H. 1999. *J. Stat. Phys.* 95:333
15. Ge H, Qian M, Qian H. 2012. *Phys. Rep.* 510:87



16. van den Broeck C, Esposito M. 2015. *Physica A* 418:6
17. Parrondo JMR, Horowitz JM, Sagawa T. 2015. *Nat. Phys.* 11:131
18. Martinez IA, Roldan E, Dinis L, Petrov D, Parrondo JMR, Rica RA. 2016. *Nat. Phys.* 12:67
19. Ciliberto S. 2017. *Phys. Rev. X* 7:021051
20. Marsland R III, England J. 2018. *Rep. Prog. Phys.* 81:016601
21. Gnesotto F, Mura F, Gladrow J, Broedersz CP. 2018. *Rep. Prog. Phys.* 81:066601
22. Alemany A, Ribezzi-Crivellari M, Ritort F. 2015. *New J. Phys.* 17:075009
23. Garcia-Garcia R, Lahiri S, Lacoste D. 2016. *Phys. Rev. E* 93:032103
24. Talkner P, Hänggi P. 2016. *Phys. Rev. E* 94:022143
25. Seifert U. 2016. *Phys. Rev. Lett.* 116:020601
26. Jarzynski C. 2017. *Phys. Rev. X* 7:011008
27. Strasberg P, Esposito M. 2017. *Phys. Rev. E* 95:062101
28. Miller HJD, Anders J. 2017. *Phys. Rev. E* 95:062123
29. Aurell E. 2018. *Phys. Rev. E* 97:042112
30. van Kampen NG. 1981. *Stochastic Processes in Physics and Chemistry*. Amsterdam: North-Holland
31. Maes C, Netocný K. 2003. *J. Stat. Phys.* 110:269
32. Seifert U. 2011. *Eur. Phys. J. E* 34:26
33. Schnakenberg J. 1976. *Rev. Mod. Phys.* 48:571
34. Puglisi A, Sarracino A, Vulpiani A. 2017. *Phys. Rep.* 709–710:1
35. Dieterich E, Camunas-Soler J, Ribezzi-Crivellari M, Seifert U, Ritort F. 2015. *Nat. Phys.* 11:971
36. Falasco G, Baiesi M. 2016. *New J. Phys.* 18:043039
37. Esposito M. 2012. *Phys. Rev. E* 85:041125
38. Cover TM, Thomas JA. 2006. *Elements of Information Theory*. Hoboken, NJ, and Canada: John Wiley & Sons, 2nd ed.
39. Kawai R, Parrondo JMR, van den Broeck C. 2007. *Phys. Rev. Lett.* 98:080602
40. Gomez-Marin A, Parrondo JMR, van den Broeck C. 2008. *Phys. Rev. E* 78:011107
41. Parrondo JMR, van den Broeck C, Kawai R. 2009. *New J. Phys.* 11:073008
42. Vaikuntanathan S, Jarzynski C. 2009. *Europhys. Lett.* 87:60005
43. Blythe RA. 2008. *Phys. Rev. Lett.* 100:010601
44. Roldan E, Parrondo JMR. 2010. *Phys. Rev. Lett.* 105:150607
45. Roldan E, Parrondo JMR. 2012. *Phys. Rev. E* 85:031129
46. Muy S, Kundu A, Lacoste D. 2013. *J. Chem. Phys.* 139:124109
47. Kawaguchi K, Nakayama Y. 2013. *Phys. Rev. E* 88:022147
48. Mehl J, Lander B, Bechinger C, Blickle V, Seifert U. 2012. *Phys. Rev. Lett.* 108:220601
49. Pietzonka P, Zimmermann E, Seifert U. 2014. *Europhys. Lett.* 107:20002
50. Uhl M, Pietzonka P, Seifert U. 2018. *J. Stat. Mech.: Theor. Exp.* 2018:023203
51. Knoch F, Speck T. 2015. *New J. Phys.* 17:115004
52. Puglisi A, Pigolotti S, Rondoni L, Vulpiani A. 2010. *J. Stat. Mech.: Theor. Exp.* 2010:P05015
53. Bo S, Celani A. 2014. *J. Stat. Phys.* 154:1325
54. Rahav S, Jarzynski C. 2007. *J. Stat. Mech.: Theor. Exp.* 2007:P09012
55. Wang SW, Kawaguchi K, Sasa Si, Tang LH. 2016. *Phys. Rev. Lett.* 117:070601
56. Harada T, Sasa S. 2005. *Phys. Rev. Lett.* 95:130602
57. Hartich D, Barato AC, Seifert U. 2014. *J. Stat. Mech.: Theor. Exp.* 2014:P02016
58. Horowitz JM, Esposito M. 2014. *Phys. Rev. X* 4:031015
59. Shiraishi N, Sagawa T. 2015. *Phys. Rev. E* 91:012130
60. Bisker G, Polettini M, Gingrich TR, Horowitz JM. 2017. *J. Stat. Mech.: Theor. Exp.* 2017:093210
61. Zimmermann E, Seifert U. 2015. *Phys. Rev. E* 91:022709
62. Romanczuk P, Bär M, Ebeling W, Lindner B, Schimansky-Geier L. 2012. *Eur. Phys. J. Spec. Top.* 202:1
63. Cates ME. 2012. *Rep. Prog. Phys.* 75:042601
64. Marchetti MC, Joanny JF, Ramaswamy S, Liverpool TB, Prost J, et al. 2013. *Rev. Mod. Phys.* 85:1143
65. Elgeti J, Winkler RG, Gompper G. 2015. *Rep. Prog. Phys.* 78:056601
66. Cates ME, Tailleur J. 2015. *Ann. Rev. Condens. Matter Phys.* 6:219

67. Prost J, Jülicher F, Joanny JF. 2015. *Nat. Phys.* 11:111
68. Bialké J, Speck T, Löwen H. 2015. *J. Non-Cryst. Solids* 407:367
69. Marconi UMB, Maggi C. 2015. *Soft Matter* 11:8768
70. Bechinger C, Di Leonardo R, Löwen H, Reichhardt C, Volpe G, Volpe G. 2016. *Rev. Mod. Phys.* 88:045006
71. Oshanin G, Popescu MN, Dietrich S. 2017. *J. Phys. A: Math. Theor.* 50:134001
72. Illien P, Golestanian R, Sen A. 2017. *Chem. Soc. Rev.* 46:5508
73. Ramaswamy S. 2017. *J. Stat. Mech.: Theor. Exp.* 2017:054002
74. Fodor E, Nardini C, Cates ME, Tailleur J, Visco P, van Wijland F. 2016. *Phys. Rev. Lett.* 117:038103
75. Mandal D, Klymko K, DeWeese MR. 2017. *Phys. Rev. Lett.* 119:258001
76. Jülicher F, Prost J. 2009. *Eur. Phys. J. E* 29:27
77. Yan W, Brady JF. 2015. *Soft Matter* 11:6235
78. Pietzonka P, Seifert U. 2018. *J. Phys. A: Math. Theor.* 51:01LT01
79. Gaspard P, Kapral R. 2017. *J. Chem. Phys.* 147:211101
80. Speck T. 2016. *Europhys. Lett.* 114:30006
81. Ganguly C, Chaudhuri D. 2013. *Phys. Rev. E* 88:032102
82. Chaudhuri D. 2014. *Phys. Rev. E* 90:022131
83. Szamel G. 2014. *Phys. Rev. E* 90:012111
84. Speck T. 2017. *Europhys. Lett.* In press. arXiv:1707.05289
85. Puglisi A, Marconi UMB. 2017. *Entropy* 19:356
86. Wu XL, Libchaber A. 2000. *Phys. Rev. Lett.* 84:3017
87. Chen DTN, Lau AWC, Hough LA, Islam MF, Goulian M, et al. 2007. *Phys. Rev. Lett.* 99:148302
88. Maggi C, Paoluzzi M, Pellicciotta N, Lepore A, Angelani L, Di Leonardo R. 2014. *Phys. Rev. Lett.* 113:238303
89. Argun A, Soni J, Dabelow L, Bo S, Pesce G, et al. 2017. *Phys. Rev. E* 96:052106
90. Krishnamurthy S, Ghosh S, Chatterji D, Ganapathy R, Sood AK. 2016. *Nat. Phys.* 12:1134
91. Schmiedl T, Seifert U. 2008. *Europhys. Lett.* 81:20003
92. Blickle V, Bechinger C. 2012. *Nat. Phys.* 8:143
93. Zakine R, Solon A, Gingrich T, van Wijland F. 2017. *Entropy* 19:193
94. Steffenoni S, Kroy K, Falasco G. 2016. *Phys. Rev. E* 94:062139
95. Barato AC, Seifert U. 2015. *Phys. Rev. Lett.* 114:158101
96. Gingrich TR, Horowitz JM, Perunov N, England JL. 2016. *Phys. Rev. Lett.* 116:120601
97. Barato AC, Seifert U. 2016. *Phys. Rev. X* 6:041053
98. Pietzonka P, Barato AC, Seifert U. 2016. *J. Stat. Mech.: Theor. Exp.* :124004
99. Seifert U. 2018. *Physica A* 504:176
100. Visscher K, Schnitzer M, Block SM. 1999. *Nature* 400:184
101. Hwang W, Hyeon C. 2018. *J. Phys. Chem. Lett.* 9:513
102. Pietzonka P, Seifert U. 2018. *Phys. Rev. Lett.* 120:190602
103. Pietzonka P, Ritort F, Seifert U. 2017. *Phys. Rev. E* 96:012101
104. Horowitz JM, Gingrich TR. 2017. *Phys. Rev. E* 96:020103
105. Pietzonka P, Barato AC, Seifert U. 2016. *Phys. Rev. E* 93:052145
106. Gingrich TR, Rotskoff GM, Horowitz JM. 2017. *J. Phys. A: Math. Theor.* 50:184004
107. Pietzonka P, Barato AC, Seifert U. 2016. *J. Phys. A: Math. Theor.* 49:34LT01
108. Polettini M, Lazarescu A, Esposito M. 2016. *Phys. Rev. E* 94:052104
109. Barato AC, Seifert U. 2015. *J. Phys. Chem. B* 119:6555
110. Nardini C, Touchette H. 2018. *Eur. Phys. J. B* 91:16
111. Dechant A, Sasa S. 2018. *J. Stat. Mech.: Theor. Exp.* 2018:063209
112. Fischer LP, Pietzonka P, Seifert U. 2018. *Phys. Rev. E* 97:022143
113. Maes C. 2017. *Phys. Rev. Lett.* 119:160601
114. Brandner K, Hanazato T, Saito K. 2018. *Phys. Rev. Lett.* 120:090601
115. Barato AC, Seifert U. 2017. *New J. Phys.* 19:073021
116. Machta BB. 2015. *Phys. Rev. Lett.* 115:260603



117. Proesmans K, van den Broeck C. 2017. *Europhys. Lett.* 119:20001
118. Shiraishi N. 2017. arXiv:1706.00892
119. Chiuchiù D, Pigolotti S. 2018. *Phys. Rev. E* 97:032109
120. Brandner K, Saito K, Seifert U. 2015. *Phys. Rev. X* 5:031019
121. Esposito M, Parrondo JMR. 2015. *Phys. Rev. E* 91:052114
122. Raz O, Subasi Y, Jarzynski C. 2016. *Phys. Rev. X* 6:021022
123. Rotskoff GM. 2017. *Phys. Rev. E* 95:030101
124. Ray S, Barato AC. 2017. *Phys. Rev. E* 96:052120
125. Macieszczak K, Brandner K, Garrahan JP. 2018. *Phys. Rev. Lett.* 121:130601
126. Garrahan JP. 2017. *Phys. Rev. E* 95:032134
127. Ray S, Barato AC. 2017. *J. Phys. A: Math. Theor.* 50:355001
128. Saito K, Dhar A. 2016. *Europhys. Lett.* 114:50004
129. Gingrich TR, Horowitz JM. 2017. *Phys. Rev. Lett.* 119:170601
130. Neri I, Roldán E, Jülicher F. 2017. *Phys. Rev. X* 7:011019
131. Pigolotti S, Neri I, Roldán E, Jülicher F. 2017. *Phys. Rev. Lett.* 119:140604
132. Barato AC, Roldán E, Martinez IA, Pigolotti S. 2018. *Phys. Rev. Lett.* 121:090601
133. Goldt S, Seifert U. 2017. *Phys. Rev. Lett.* 118:010601
134. Goldt S, Seifert U. 2017. *New J. Phys.* 19:113001
135. Lan G, Sartori P, Neumann S, Sourjik V, Tü Y. 2012. *Nat. Phys.* 8:422
136. Mehta P, Schwab DJ. 2012. *PNAS* 109:17978
137. Govern CC, ten Wolde PR. 2014. *Phys. Rev. Lett.* 113:258102
138. Hartich D, Barato AC, Seifert U. 2015. *New J. Phys.* 17:055026
139. Sartori P, Pigolotti S. 2015. *Phys. Rev. X* 5:041039
140. Bo S, Giudice MD, Celani A. 2015. *J. Stat. Mech.: Theor. Exp.* 2015:P01014
141. Mora T. 2015. *Phys. Rev. Lett.* 115:038102
142. ten Wolde PR, Becker NB, Ouldrige TE, Mugler A. 2016. *J. Stat. Phys.* 162:1395
143. Poletini M, Esposito M. 2014. *J. Chem. Phys.* 141:024117
144. Brown AI, Sivak DA. 2017. *PNAS* 114:11057
145. Nguyen B, Hartich D, Seifert U, De Los Rios P. 2017. *Biophys. J.* 113:362
146. Wang CH, Mehta P, Elbaum M. 2017. *Phys. Rev. Lett.* 118:158101
147. Ouldrige TE, Govern CC, ten Wolde PR. 2017. *Phys. Rev. X* 7:021004
148. Cao Y, Wang H, Ouyang Q, Tü Y. 2015. *Nat. Phys.* 11:772
149. Barato AC, Seifert U. 2017. *Phys. Rev. E* 95:062409
150. Nguyen M, Vaikuntanathan S. 2016. *PNAS* 113:14231